4

Molecular Interactions at Interfaces

Raj Kumar Gupta and V. Manjuladevi
Department of Physics, Birla Institute of Technology & Science, Pilani
India

1. Introduction

The study on molecular organization and structure formation at the nanometer length scale is important due to its vast application in the field of nanoscience and nanotechnology. Molecular interactions play a pivotal role in the process of molecular assembly. The properties of materials can be maneuvered precisely by manipulating the structures at the nanometer length scale. The field of thin films science and technology has been growing remarkably due to its enormous industrial applications. The properties of thin films depend on the nature of the adsorbate and the structures on the surface. The structures of the thin films on a surface leads to the growth of bulk material, and hence the material properties can be controlled by manipulating the structures of the thin films. The form of such structures depends on the molecule-substrate and intermolecular interactions. The development of thin films science and technology has influenced the field of nanoscience and nanotechnology significantly. In this chapter, we discuss the role of molecular interactions in ultrathin films at air-water (A-W) and air-solid (A-S) interfaces. We form monomolecular thick films on the surface of water and study the film stability, surface phases, and other thermodynamical parameters. We found that the stability of the films at the A-W interface primarily depends on the molecular-surface and intermolecular interaction. Amphiphilic molecules, when spread on the water surface, form a monomolecular thick film at A-W interface. Such monomolecular thick film is known as Langmuir monolayer. An amphiphilic molecule has two parts : hydrophilic (water loving) and hydrophobic (water hating) part. When such molecules with a proper balance between hydrophilic and hydrophobic parts are dispersed on water surface, the hydrophilic part gets anchored to the water surface whereas the hydrophobic part stays away from the water surface. Under such condition, the anchored molecules are constrained to move on the two dimensional smooth water surface. The surface density can be varied and a corresponding change in surface tension is recorded. A Langmuir monolayer has proved to be an ideal two dimensional system not only for studying the thermodynamics but also for depositing the films on different types of substrates by vertical deposition mechanism in a highly controlled manner. Such films at A-S interface are known as Langmuir-Blodgett (LB) films.

In this chapter, we discuss the effect of amphiphilicity (a balance between the hydrophobic and hydrophilic part of the amphiphilic molecule) on the Langmuir monolayer. We discuss the stability of Langmuir monolayer of a hydrophobic molecules (e.g. thiocholesterol) in the matrix of a very stable Langmuir film of cholesterol. The stability of such hydrophobic molecules is due to the attractive interaction between the molecule which arises due to overall gain in entropy of the system. There are few reports on the Langmuir monolayer of purely hydrophobic nanoparticles at A-W interface. Since the particles are hydrophobic, the stability of such systems are questionable. We changed the chemistry of gold nanoparticles such that it attains an amphiphilic nature. The Langmuir monolayer of such amphiphilic

gold nanoparticle (AGN) exhibited variety of surface phases like low ordered liquid phase, high ordered liquid phase, bilayer of high ordered liquid phase and a collapsed state. Based on the thermodynamical studies of Langmuir monolayer of AGN, a phase diagram has been constructed. The Langmuir films at A-W interface can be transferred to solid substrates by LB technique. Here also, the nature of aggregation and deposition depends on molecule-substrates and intermolecular interaction. Interestingly, it was found that repeated process of adsorption and partial desorption of cholesterol molecules from hydrophobic substrates lead to the formation of uniformly distributed torus shaped domains.

2. Experimental techniques

2.1 Monolayer and multilayer at air-water interface

2.1.1 Surface manometry

Surface manometry is a standard technique to study the thermodynamics and the surface phases in a Langmuir monolayer. The presence of a monolayer at the A-W interface reduces the surface tension of water. Such reduction in the surface tension is defined as surface pressure (π) (Gaines, 1966). In surface manometry, the surface density of the molecules adsorbed at the interface is varied and the surface pressure (π) is recorded at a constant temperature. This yields a surface pressure - surface density isotherm. The area per molecule (A_m) is defined as the inverse of the surface density. The instrument for the measurement of $\pi - A_m$ isotherm is shown in Figure 1. It consists of a teflon trough and barriers. The subphase was ultrapure ion-free water having a resistivity greater than 18 megaΩ-cm

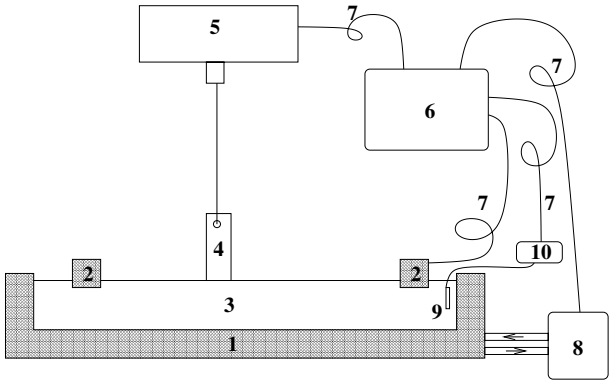

Fig. 1. A schematic diagram showing the experimental setup for the measurement of surface pressure (π) - area per molecule (A_m) isotherms. The basic parts of the setup are as follows: (1) teflon trough, (2) teflon barriers, (3) subphase (ion-free water), (4) Wilhemy plate (filter paper), (5) surface pressure sensor, (6) computer, (7) connecting wires, (8) thermostat, (9) resistance temperature detector (RTD) and (10) digital multimeter for measuring resistance

obtained by passing distilled water through filtering and deionizing columns of a Milli-Q Millipore unit. The sample was dissolved in an appropriate solvent to obtain a solution of known concentration. The solution of the samples was spread on the water subphase between the barriers using a precisely calibrated microsyringe (obtained from Hamilton). The solvent was allowed to evaporate for 15 minutes before starting the compression. The surface density of the molecules in the monolayer is varied by changing the area available

for the molecules by moving the barriers laterally. The barriers are driven by motors which are controlled by a computer. They are coupled to each other so that it ensures a symmetric compression of the monolayer. The surface pressure was measured using a Wilhemy plate method (Gaines, 1966; Adamson, 1990). We have used filter paper of appropriate size as the Wilhemy plate. The surface pressure and area per molecule at a constant temperature were recorded simultaneously using a computer. This gives the π-A_m isotherm of the spread molecule. The isotherms at different temperatures are obtained by controlling the temperature of the subphase. This was achieved by circulating water at the required temperature inside the chamber of the trough using a thermostat. The temperature of the subphase was measured by a resistance temperature detector (RTD) and a digital multimeter. A typical π - A_m isotherm is shown in Figure 2(a). A plateau in the isotherm represents the coexistence of two phases. A

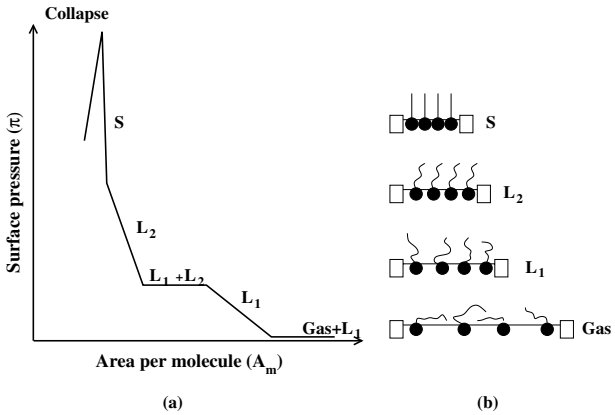

Fig. 2. (a) shows a typical isotherm indicating the different phases in a Langmuir monolayer. (b) shows the molecular arrangement in the different phases. The symbols L_1, L_2 and S represent liquid expanded, liquid condensed and solid phases, respectively

kink in the isotherm indicates a phase transition. At a very large area per molecule (A_m), the molecules are far apart and do not exert any force on each other. This is a 2D gas phase. On compression, the molecules condense to a low density liquid state (L_1). There are no positional and orientational orders in the molecules in this phase. On further compression, the L_1 phase transforms to a high density liquid state (L_2) accompanied by a two phase (L_1+L_2) coexisting region. This is known as condensed (L_2) phase. In the L_2 phase, molecules exhibit a long range orientational order and a quasi-long range positional order. On compression, the L_2 phase transforms to a 2D solid (S) phase. On further compression, the monolayer collapses. This is indicated by a sharp decrease in surface pressure.

The area per molecule at which the isotherm indicates very small and finite values of the surface pressure (*e.g.* 0.2 mN/m) is known as lift-off area per molecule (A_i). The average area occupied by the molecules in a phase is determined by extrapolating the corresponding region of the isotherm to the zero surface pressure on the A_m axis. The extrapolation of the steep region (*e.g.* S phase in Figure 2) of the isotherm to zero surface pressure is called limiting area per molecule (A_o). This is the minimum area to which the molecules can be compressed on the water surface without collapsing the monolayer. The orientational state (tilt or untilt) of the molecules in a phase can be estimated qualitatively by comparing the extrapolated area per molecule with that of molecular cross-sectional area in the bulk single crystal.

The isothermal in-plane elastic modulus E is an appropriate quantity for distinguishing very weak phase transitions. The isothermal in-plane elastic modulus Mohwald (1995) is defined as

$$E = -(A_m)\frac{d\pi}{dA_m} \tag{1}$$

The relaxation in the molecular area with time at a given surface pressure can indicate the nature of stability of the monolayer at the interface. A fast reduction in the area with time may indicate an unstable monolayer where the instability can be attributed to dissolution of the molecules to subphase or evaporation. A slow reduction can be attributed to the relaxation of the molecules in the monolayer. The nature and the mechanism of collapse can be studied by monitoring the change in molecular area with time at a constant surface pressure Smith & Berg (1980). In some special cases, kinetics of adsorption of the molecules from the subphase to the monolayer at the interface can be studied. In such cases, the area was found to increase or decrease with time due to complex formation of the molecules in the subphase with the molecules at the interface Ramakrishna et al. (2002). It provides a method to study kinetics of the surface chemistry.

The equilibrium spreading pressure (ESP) is a surface pressure of a monolayer coexisting with its bulk phase at the interface (Gaines, 1966). When a speck of crystallite is placed on the water surface, the molecules from the bulk crystallites elude out and form a monolayer at the interface spontaneously. After a certain period of time, the system reaches an equilibrium state where the rate of elution of molecules from the crystallites is equal to the rate of molecules binding to the crystallites. The variation in surface pressure with time shows an initial increase in surface pressure due to the formation of monolayer. On reaching the equilibrium, the surface pressure value saturates. The saturated value of surface pressure is known as ESP. The studies on ESP indicate the spreading capability of the molecules at an interface (Gaines, 1966). The finite value of ESP can suggest the monolayer to be stable against dissolution or evaporation of the molecules. The ESP values of some molecules like stearic acid, octadecanol and dipalmitoyl phosphatidylcholine are 5.2, 34.3 and 1 mN/m, respectively Smith & Berg (1980).

There are many two dimensional systems in nature that occur in mixed state. For instance, a bio-membrane constitutes of various kind of phospholipids, cholesterol and fatty acids. The Langmuir monolayer of phospholipids mimic the biological membranes and has been extensively studied (Mohwald, 1995). The stability and miscibility of the component molecules will be studied by estimating the excess Gibbs free energy of the system. For an ideal case of complete miscibility or immiscibility of two-component monolayer system, the area of the mixed monolayer is given by the rule of additivity,

$$A_{id} = A_1X_1 + A_2X_2 \tag{2}$$

where X_1 and X_2 are the mole fractions of the components 1 and 2, respectively. A_1 and A_2 are the A_m of the individual pure component monolayers. However, for a mixed system, the monolayer area can deviate from the ideal case. Such deviation in the monolayer area depends on the nature of the interaction between the component molecules and is known as the excess area per molecule, A_{ex}. The A_{ex} is defined as

$$A_{ex} = A_{12} - A_{id} \tag{3}$$

where A_{12} is the experimentally determined values of the A_m of the mixed monolayer. A_{id} is the ideal A_m value calculated from Equation 2. The positive or the negative value of the

A_{ex} indicates a repulsive or an attractive interaction, respectively between the component molecules in the mixed monolayer.

The stability and the degree of miscibility of a mixed monolayer were studied by calculating the excess Gibbs free energy (ΔG) Goodrich (1957); Seoane et al. (2001). The ΔG is given by

$$\Delta G = N_a \int_0^{\pi} A_{ex} d\pi \tag{4}$$

where N_a is the Avogadro number and π is the surface pressure. The negative or positive values of ΔG indicate stable or unstable mixed monolayer system respectively.

2.1.2 Epifluorescence microscopy

In 1981, Tscharner and McConnell Tscharner & McConnell (1981) have developed the epifluorescence microscopy technique to visualize a monomolecular layer at the A-W interface. The schematic diagram of the experimental setup for the epifluorescence microscopy of the Langmuir monolayer is shown in Figure 3. Here, the monolayer (S) was doped with very small quantity ($\leq$ 1 mole%) of an amphiphilic fluorescent dye molecule (D). The dye doped monolayer was observed under an epifluorescence microscope (Leitz Metallux 3). The microscope was equipped with a high pressure mercury lamp (H) and a filter block (F). The filter block consists of an emission filter (Em), an excitation filter (Ex) and a dichroic mirror (DM). The excitation filter allows the light of appropriate wavelength to excite the dye molecules in the monolayer. The reflected light from the interface and emitted light from the dye doped monolayer was allowed to pass through the emission filter (Em) which allows only the emitted light. The emitted light was collected using an intensified charge coupled device camera (ICCD) and the images were digitized using a frame grabber (National Instruments, PCI-1411). The intensity of the emitted light depends on the miscibility of the dye molecules in a particular phase of the monolayer. The gas phase appears dark due to the quenching of the dye molecules. The liquid expanded phase appears bright in the epifluorescence images. On the other hand, the solid phase appears dark. This is due to the expulsion of dye molecules from the highly dense solid domains. In all the epifluorescence microscopy experiments, we have utilized 4-(hexadecylamino)-7-nitrobenz-2 oxa-1,3 diazole (obtained from Molecular Probes) as an amphiphilic fluorescent molecule.

2.1.3 Brewster angle microscopy

The epifluorescence microscopy on the Langmuir monolayer has certain disadvantages. For instance, the fluorescent dye acts as an impurity and may alter the phase diagram. There are difficulties in determining the surface phases at the higher surface pressures where the dye molecules are practically insoluble in the domains. Also the photo-bleaching can result in the decomposition of the dye molecules. To overcome such disadvantages, a microscope which works on the principle of Brewster angle, was developed. The microscope is known as the Brewster angle microscope Hönig & Möbius (1991); Hénon & Meunier (1991). The angle of incidence at which an unpolarized light acquires a linearly polarized state after reflection from the plane of an interface is known as Brewster angle of the reflecting material. The state of polarization of the reflected light at the Brewster angle (θ_B) is perpendicular (s-polarized) to the plane of incidence. At Brewster angle of incidence

$$tan(\theta_B) = n_2/n_1 \tag{5}$$

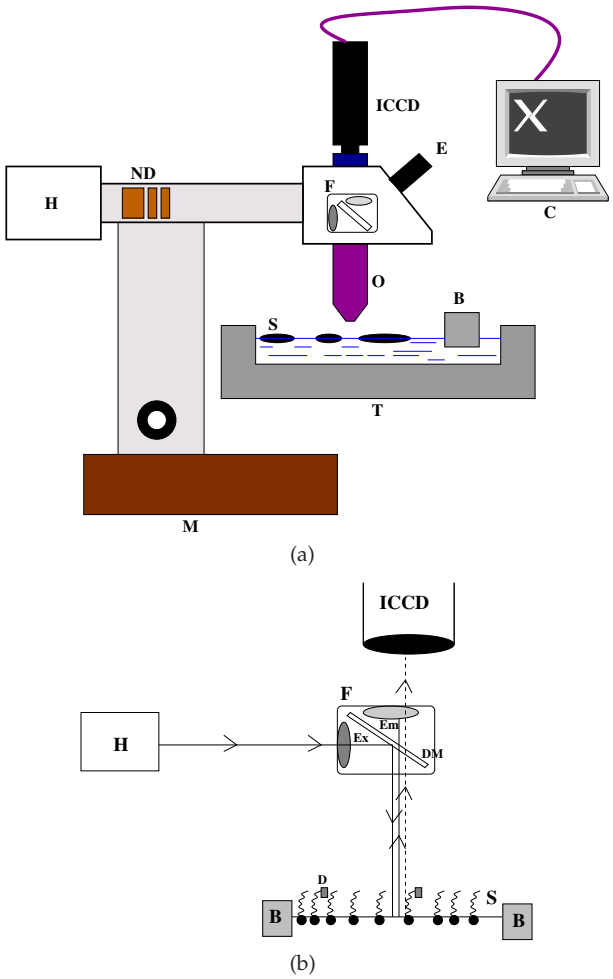

Fig. 3. Schematic diagram showing the experimental setup for the epifluorescence microscopy. (a) shows a complete microscope setup. (b) shows the working principle of the microscope. The different parts are as follows: high pressure mercury lamp (H), neutral density filter (ND), filter block (F) with emission (Em) and excitation (Ex) filters and a dichroic mirror (DM), objective (O), eye-piece (E), microscope stand (M), intensified charge coupled device (ICCD) camera, computer (C), trough (T), dye doped monolayer (S), dye molecule (D) and barrier (B)

where n_2 is the refractive index of the reflecting material and n_1 is the refractive index of the medium through which the light is incident. We have utilized a commercial setup, MiniBAM Plus from Nanofilm Technologie for BAM imaging. In the microscope, a polarized light source from a 30 mW laser of wavelength 660 nm falls on the water surface at the Brewster angle ($\sim$53°). The reflected light is allowed to pass through a polarizer which allows only the p-component of the reflected light to enter a CCD camera, as shown in Figure 4. Since the

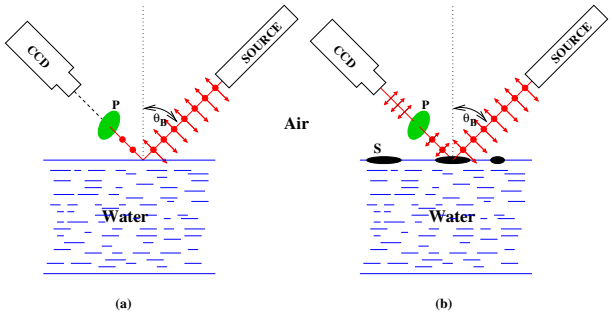

Fig. 4. Schematic diagrams showing the working principle of a Brewster angle microscope. θ_B is the Brewster angle of water with respect to air. The different parts are as follows: polarizer (P), charge coupled device (CCD) camera and monolayer at the air-water interface (S). (a) and (b) are the BAM setups without and with monolayer at the A-W interface, respectively

angle was set for the Brewster angle of water, the reflected intensity in the CCD camera was minimum for pure water. Therefore, any domain of the monolayer changes the refractive index at the interface and hence the Brewster angle for A-W interface gets altered. This in turn reflects some light which was collected by the CCD to form the images of the monolayer domains. The intensity of the reflected light depends on the thickness of the film and the surface density of the molecules. The optical anisotropy in the BAM images arises due to a difference in tilt-azimuth variation of the molecules in the monolayer and the anisotropy in the unit cell Rivière et al. (1994).

2.2 Monolayer and multilayer at air-solid interface

Langmuir-Blodgett (LB) technique can be employed to form monolayer or multilayer films at the solid-air interface. In this technique, the monolayer in a particular phase at the A-W interface can be transferred layer by layer onto a solid substrate by vertically moving the substrate in and out of the subphase. During deposition, the surface pressure is fixed at some target value known as target surface pressure (π_t). The experimental setup for LB deposition is shown in Figure 5. The setup is similar to that of the Langmuir trough except it possesses a well in the teflon trough and a dipper. For the LB film transfer, the trough has a motorized dipper which holds the substrate and it can be moved up and down very precisely. Such a motion makes the substrate to dip in and out of the subphase with a monolayer at the interface. During deposition, the surface pressure is fixed at π_t by a feedback mechanism. The barriers compress the monolayer until the π_t is attained. Any increase or decrease in surface pressure is fed back to the computer which in turn moves the barrier to maintain the required target surface pressure. The mechanism of building multilayer by LB technique is shown in Figure 6(a). The efficiency of transfer of the monolayer on the solid substrate is estimated by measuring the transfer ratio (τ). The transfer ratio (τ) is defined as Roberts (1990)

$$\tau = \frac{\text{area of monolayer transferred from the A} - \text{W interface}}{\text{area of the substrate to be deposited}} \tag{6}$$

The value of τ equal to one indicates defectless LB film. There are different types of LB deposition. If the monolayer transfers during both the upstroke and downstroke of the dipper, such deposition is known as Y-type of LB deposition. On the other hand, if the deposition

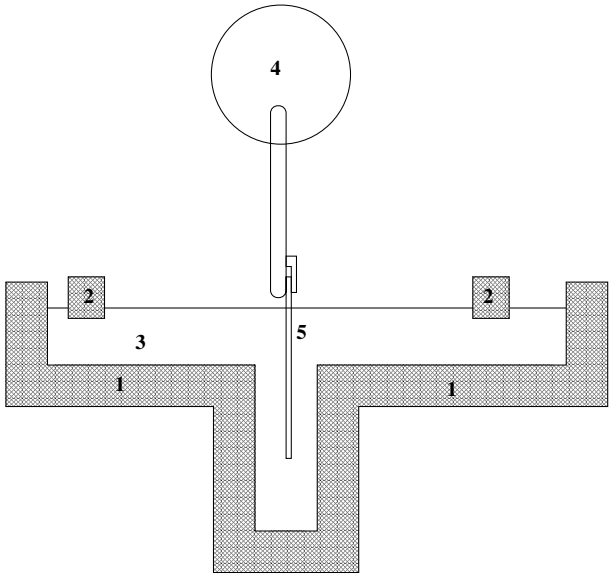

Fig. 5. A schematic diagram showing the experimental setup for forming Langmuir-Blodgett films. The parts are as follows: (1) teflon trough with a well in the center, (2) barriers, (3) subphase, (4) dipper and (5) substrate

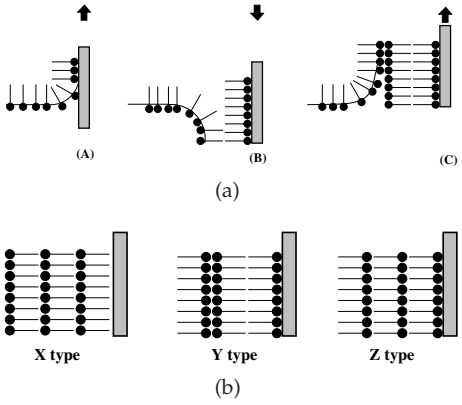

Fig. 6. (a) depicts the mechanism of formation of multilayer by the Langmuir-Blodgett technique. (A) first upstroke, (B) first downstroke and (C) second upstroke. (b) shows the structure of different types of multilayer obtained by LB technique, namely X-, Y- and Z-type

takes place only with either downstrokes or upstrokes, they are termed as X or Z-type of LB deposition, respectively (Figure 6(b)). Sometimes a combination of these depositions are also observed Roberts (1990). The negative values of τ indicate desorption. The LB depositions are dependent on the nature of interaction between the substrate and the molecules, dipper speed, target surface pressure, ion contents of the subphase and temperature. We have employed a

Langmuir-Blodgett trough procured commercially from NIMA (model 611M) for both surface manometry studies and LB film deposition.

The monolayer at the A-W interface can be transferred onto substrates by two other different techniques. These are called horizontal transfer method and Schaefer's method. In the horizontal transfer method, the substrate is immersed horizontally in the subphase and then the monolayer is formed at the A-W interface. Then the aqueous subphase is siphoned out very slowly from the other side of the barriers. The monolayer gets adsorbed onto the substrate as the water drains out. In the Schaefer's method, a hydrophobic substrate is allowed to touch the monolayer on the water surface. The hydrophobic part of the molecules get adsorbed to the substrate. To facilitate the drainage of water, the substrates in either case can be tilted by a small angle prior to the adsorption.

2.2.1 Scanning probe microscopy

The discovery of scanning probe microscopes by Binning and coworkers has revolutionized the field of nanoscience and nanotechnology. Its versatile range of applications have made it an indispensable tool in the fields of surface science and other branches of soft condensed matter. It is useful in the study of the surface topography, electronic properties of the film, film growth, adhesion, friction, lubrication, dielectric and magnetic properties. It has also been used in a molecular or atomic manipulation. Among the various scanning probe microscopes, scanning tunneling Binning et al. (1982) and atomic force microscopes Binning et al. (1986) are widely used to study nanostructures in thin films.

The schematic diagram of the STM is shown in Figure 7. In scanning tunneling microscope, a very sharp metallic tip (T) is brought very close to a conducting substrate (S). The substrate may be coated with a film (F). When a low bias voltage ($\sim$1 V) is applied between the tip and the substrate, a tunneling current flows between them. STM works in two modes $-$ constant current (CC) mode and constant height (CH) mode. While scanning the surface in CC mode, the tunneling current between the tip and the sample is kept constant. In this mode, the height of the tip is adjusted automatically using a feedback circuit to achieve the constant tunneling current. The variation in tip height (z) as a function of lateral coordinates (x,y) gives the topographic information of the sample. In CH mode, the height of the tip is kept constant and the tunneling current is recorded as a function of (x,y). The CH mode provides the electronic information of the sample. Atomic force microscope (AFM) gives the topographic images by sensing the atomic forces between a sharp tip and the sample. A schematic diagram of an AFM is shown in Figure 8. Here, the tip is mounted on a cantilever. The head of the tip is coated with a reflecting material like gold and it is illuminated by a laser light. The reflected light is collected on a quadrant photodiode. Any deflection in the tip due to its interaction with the sample is monitored by measuring a distribution of light intensity in the photodiode. There are numerous modes of operation of AFM. In contact mode, the tip is brought into direct contact with sample and the surface is scanned. It is also known as constant force mode. Here, the force between the tip and the sample is kept constant and by monitoring the bending of the cantilever as a function of (x,y), a topographic image can be obtained. In tapping mode, the tip is allowed to oscillate nearly to its resonant frequency on the sample at a given amplitude and frequency. Due to interaction between the tip and the sample, the amplitude and phase of oscillation of the tip change. The change in amplitude can be used to obtain a topographic map of the sample. The phase change gives an insight about the chemical nature of the sample.

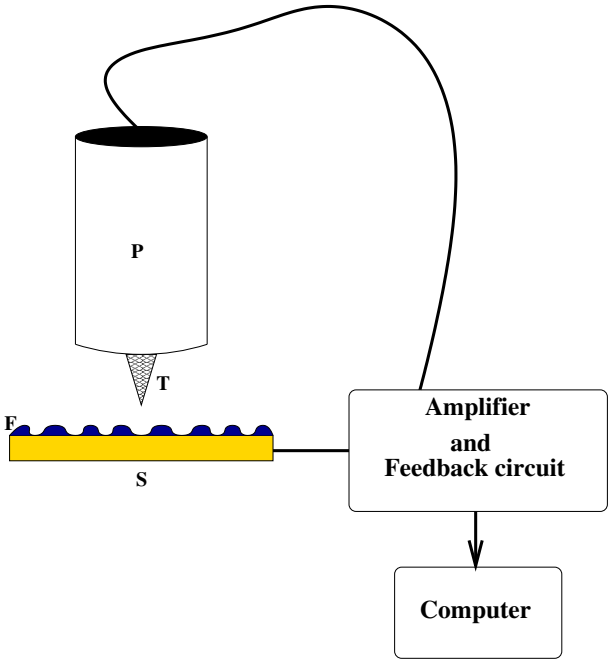

Fig. 7. Schematic diagram of a scanning tunneling microscope (STM). The parts are as follows: conducting substrate (S), film (F), metallic tip (T) and piezo tube (P)

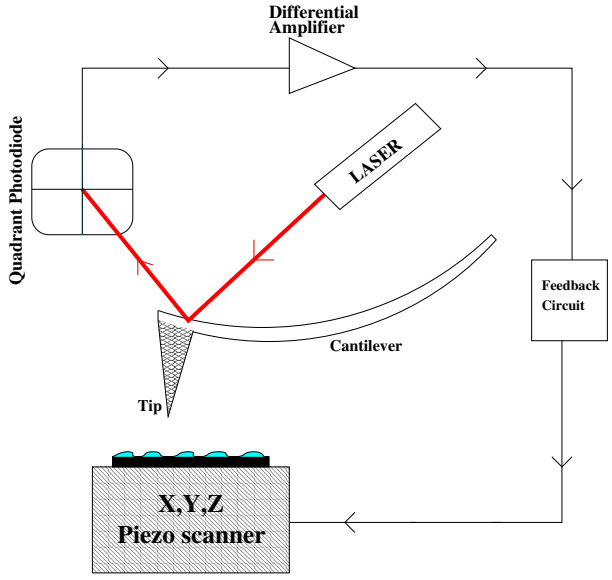

Fig. 8. Schematic diagram of an atomic force microscope (AFM)

3. Molecular interaction at air-water interface

An amphiphilic molecule has two parts : 1) hydrophilic headgroups like acid (-COOH), alcohol (-OH), amine(-NH_2) or ketone and 2) hydrophobic tail part like saturated or unsaturated aliphatic chain, and cyclic rings. The stability of the Langmuir monolayer at A-W interface essentially depends on the intermolecular and molecular - subphase interactions. In a stable Langmuir monolayer, the molecules get adsorbed to an A-W interface thereby reduces the surface energy. The energy at the air-water interface is reduced as the polar headgroups can form hydrogen bonds easily with the water molecules. The strength of molecular anchoring to the water surface depends on the nature of molecular interaction at the interface. The polar headgroups can interact with each other by coulombic, dipolar and hydrophobic interactions.

The stability of a monolayer at A-W interface depends on the nature of the aqueous subphase and the amphiphilic balance of the molecules. The Langmuir monolayer fatty acid are known to exhibit several phases. The isotherms of octadecanoic acid ($C_{17}H_{35} - COOH$), octadecanol ($C_{18}H_{37} - OH$), octadecanthiol ($C_{18}H_{37} - SH$), and octadecylamine ($C_{18}H_{37} - NH_2$) are shown in Figure 9. All the isotherms were obtained under the similar experimental conditions. In the present case, the molecules differs only in its hydrophilic headgroups. The polarity

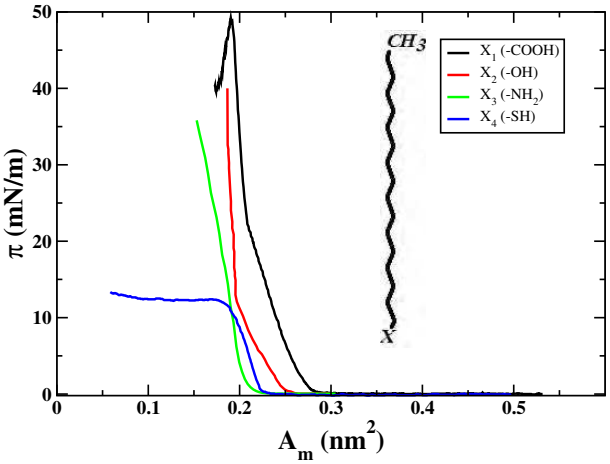

Fig. 9. Isotherms of Langmuir monolayer of octadecanol, octadecanoic acid, octadecylamine, and octadecanethiol

of the headgroups of these molecules can be arranged in decreasing order as : $-OH \rightarrow -COOH \rightarrow -NH_2 \rightarrow -SH$. The significant effect of polarity of the headgroups can be observed from the isotherms. The monolayer of the molecules with highly polar headgroup is more compressible before it collapses as compared to the molecules with lower polarity in the headgroups. The variation of isothermal inplane elastic modulus (E) as a function of A_m of above molecules are shown in Figure 10. The maximum values of E in the condensed state for X being -OH, -COOH, -NH_2 and -SH were found to be 475, 380, 175 and 80 mN/m respectively. This indicates that due to increase in polarity of headgroups of the amphiphilic molecules at the A-W interface, the condensed phase exhibits a higher degree of crystallinity.

The hydrophobic interaction between the molecules also plays a significant role in stabilizing the Langmuir monolayer. Such hydrophobic interaction arises due to an overall increase

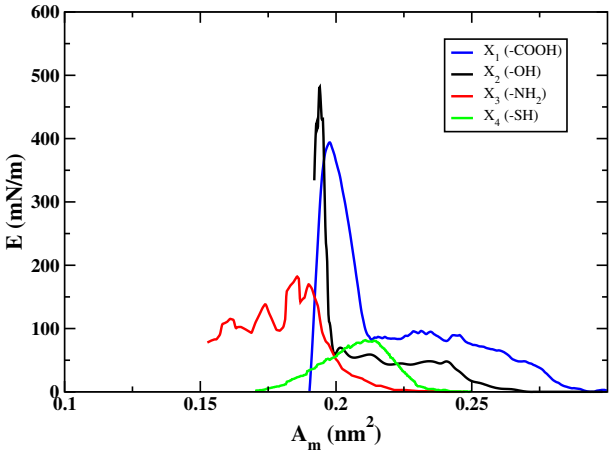

Fig. 10. Inplane elastic modulus *E* Vs A_m of octadecanol, octadecanoic acid, octadecylamine, and octadecanethiol.

in entropy of the system leading to an stabilization effect on the monolayer. It has been observed that monolayer of even pure hydrophobic materials can be stabilized provided the overall entropy increases. In some special cases, purely hydrophobic materials are also known to form a stable Langmuir monolayer Tabe et al. (2002). For instance, semifluorinated alkanes being purely hydrophobic molecules, show a stable Langmuir monolayer at the A-W interface Gaines (1991); Abed et al. (2002). The formation of such monolayers are attributed to the hydrophobic interaction between the molecules and the increase in overall entropy of the system. There is also a report on the formation of a non-traditional Langmuir monolayer of disubstituted urea lipid molecule where the hydrophilic part stays away from the water surface, whereas the hydrophobic part stays near to the water surface. The stabilization of such monolayer was attributed to the hydrogen bonding network of the urea moiety of the molecule Huo et al. (2000).

In an interesting work, we tried to stabilize hydrophobic analogous of cholesterol (Ch) molecules known as thiocholesterol (TCh) at the A-W interface. The stability of the TCh monolayer is improved by incorporating them in Ch monolayer matrix. Thiocholesterol is predominantly a hydrophobic molecule which can be obtained by the substitution of -OH group with -SH group in the cholesterol molecule. The -SH group is weakly acidic, and the amphipilicity of the TCh is not sufficient enough to form a stable Langmuir monolayer. There is a report on the formation of defect rich self assembled monolayer (SAM) of TCh on gold substrate (yang et al., 1996). The size of the defects were found to be of the order of 5-8 Å. Such defect rich SAM can be utilized for the fabrication of ultramicroelectodes selective permeation devices. It can also be used for electroanalytical and biosensors applications. However, the limitation of the formation of SAM of such organosulfur compounds is the substrate which has to be of coinage metals like gold, silver and copper. Another method of obtaining monolayer and multilayer on different types of substrate is LB technique. Hence, the formation of a stable Langmuir monolayer is important for the formation of controlled and organized LB films. It is well known that the Ch molecules form a stable monolayer at the A-W interface Slotte & Mattjus (1995); Lafont et al. (1998). Though -SH group is weakly acidic in nature Bilewicz & Majda (1991), the amphiphilic balance of the TCh for the formation of a

stable insoluble monolayer at the A-W interface is not sufficient. The TCh molecule is mostly hydrophobic in nature and does not spread to form a monolayer at the A-W interface. Since the hydrophobic skeletons of the TCh and Ch molecules are identical, TCh molecules can be mixed to the Ch monolayer and can be transferred on to different substrates by LB technique. There are numerous reports in literature indicating the formation of mixed monolayer of a non-amphiphilic component doped into the monolayer of amphiphilic molecules (Silva et al., 1996; Wang et al., 2000; Viswanath & Suresh, 2004). In all these cases, the monolayer has been stabilized upto certain value of surface pressure due to hydrophobic interaction of the tail groups of the different components. Further compression leads to the squeezing out of the non-amphiphilic components. In this work we reported that the mixed monolayer to be stable upto 0.75 mole fraction of TCh in the Ch monolayer. Our analysis of the excess area per molecule for the mixed monolayer system suggests that the monolayer is stabilized by attractive interaction between the Ch and TCh molecules.

The surface pressure (π) - area per molecule (A_m) isotherms for the different mole fractions of TCh in the mixed monolayer of Ch and TCh (X_{TCh}) are shown in Figure 11. The isotherm of

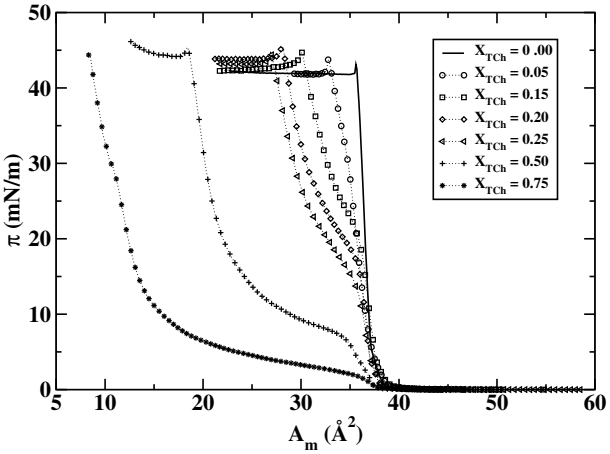

Fig. 11. The surface pressure (π) - area per molecule (A_m) isotherms of the mixed monolayer for different mole fractions of thiocholesterol in cholesterol (X_{TCh}). Reprinted with permission. (Gupta & Suresh, 2008)

pure cholesterol indicates the coexistence of a gas and an untilted condensed (L_2) phase at a large A_m Lafont et al. (1998); Viswanath & Suresh (2003). At an A_m of 39 Å^2, there is a steep rise in the surface pressure indicating a transition from the coexistence of gas and L_2 phases to the L_2 phase. The limiting area per molecule (A_o) is equal to 38 Å^2. This value approximately corresponds to the cross-sectional area of the Ch molecule for its normal orientation at the A-W interface. The monolayer collapses at an A_m of 37 Å^2 with a collapse pressure of 43 mN/m. The Ch monolayer shows a spike-like collapse and a plateau thereafter. The TCh molecules are predominantly hydrophobic in nature, and they do not spread at the A-W interface to form a stable Langmuir monolayer. We have attempted to form the TCh monolayer on different subphases obtained by changing the pH and adding salts in the ultrapure ion-free water. However, we were not able to form a stable TCh monolayer over such aqueous subphases. We have mixed the TCh and Ch molecules at different proportions, and formed the monolayer at the A-W interface. The isotherms of the mixed monolayer (Figure 11) show a sharp rise in

surface pressure at around 39 Å^2. However, the presence of TCh in Ch monolayer changes the nature of the isotherm by introducing an additional change in slope of the isotherms. Such change in slope can be considered as an initial collapse of the two-component monolayer system. The isotherms also show a final collapse. The final collapse of the mixed monolayer reveals spike-like feature followed by a plateau. This is characteristic of the collapse for the cholesterol monolayer. Hence, the final collapse indicates a collapse of the Ch rich monolayer. The A_o values for the mixed monolayer were found to be nearly invariant with X_{TCh}. It lies in the range of 37.5 - 38.5 Å^2. The values of A_o for various X_{TCh} suggest a normal orientation of the molecules in the phase corresponding to the steep region of the isotherms (Figure 11). This phase may represent untilted condensed (L_2) phase.

For an ideal case of the two-component system of non-interacting molecules, the area per molecule of the mixed monolayer is a given in Equation 2. If one of the components is a non-amphiphilic molecule (for instance component 2), then the Equation 2 can be modified as

$$A_{id} = X_1 A_1 = (1 - X_2) A_1 \tag{7}$$

The variation of excess area per molecule (A_{ex}) as a function of mole fraction of TCh in Ch for different surface pressures are shown in Figure 12. The values of A_{ex} are negative for all the compositions. The negative values of A_{ex} suggest an attractive interaction between the Ch and TCh molecules in the mixed monolayer. Such attractive interaction leads to a stabilization effect on the mixed monolayer of Ch and TCh.

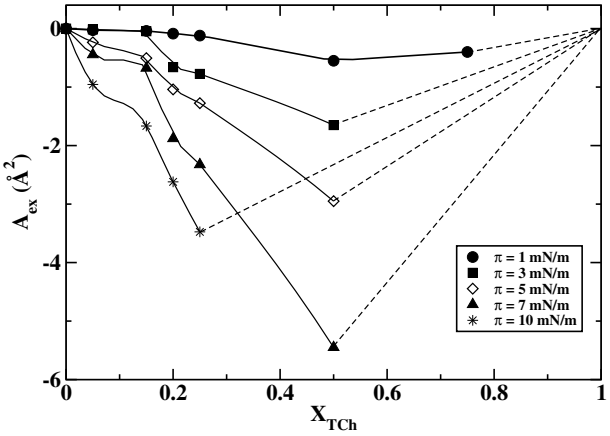

Fig. 12. Variation of excess area per molecule (A_{ex}) with respect to the mole fraction of TCh in Ch (X_{TCh}) at different surface pressures (π). The points are computed using Equation 3. The dashed lines are extrapolated to the zero value of the excess area for the pure TCh. Reprinted with permission. (Gupta & Suresh, 2008)

There are many reports on pure hydrophobic materials forming a stable monolayer at the A-W interface Tabe et al. (2002); Li et al. (1994). Tabe *et al* Tabe et al. (2002) have reported the formation of condensed monolayer of pure hydrophobic mesogenic molecules at the A-W interface. They attributed the stability of the monolayer to the gain in entropy on adsorption of the molecules at the interface. Li *et al* Li et al. (1994), have suggested that the stability of purely hydrophobic materials like a long chain alkane can be due to the van der Waals force. There is another report which indicated the stability of the monolayers of alkanes at the A-W interface.

This has been attributed to the gain in entropy due to strong fluctuations of the alkanes on a plane normal to interface as compared to their states in the bulk solid Tkachenko & Rabin (1996). Further, there are possibilities for the gain in entropy due to the rearrangement of the interfacial water molecules, and the fluctuation of the molecules as compared to their state in the bulk solids. Jensen *et al*. Jensen et al. (2003; 2004), have shown experimentally and also by simulation that the orientation of interfacial water molecules changes differently due to the presence of hydrophobic or hydrophilic molecule at the interface. The dipole moment associated with the water molecule faces on an average towards the hydrophobic alkane. However, for the hydrophilic monolayer covered interface, it faces away from the interface. In the case of mixed monolayer of Ch and TCh, we find an attractive interaction between the molecules which may arise due to the overall gain in entropy of the mixed monolayer system or due to van der Waals interaction between the molecules. In Ch - TCh mixed monolayer system, the nature of polarity of the head groups of the two mixed components are different. Hence, we can assume that each component molecules orient the interfacial water molecules differently. This will lead to a frustration in orientation of the water molecules at the interface which reduces the ordering of the interfacial water dipole moments. This increases the entropy of the system which in turn may help in stabilizing the mixed monolayer. Hence, we can assume the entropy gain in our system can be due to the reorientation of the water molecules at the interface and the fluctuations of the iso-octyl chain of the Ch and TCh molecules. On reducing the intermolecular distances by compressing the monolayer, the steric repulsion among the molecules becomes strong enough to overcome the van der Waals attraction and the entropy gain which may lead the non-amphiphilic component (*i.e*. TCh) to squeeze out of the mixed monolayer.

Because of the potential industrial applications, the field of nanoscience and nanotechnology is growing enormously. One among the major challenges involved in this area is assembly of nanomaterials such that it can exhibit extraordinary physical properties. One of the important parameters determining the properties of the nanoparticle crystals is the interparticle separation. Other parameters are charging energy of the particles, strength of interaction between the particles and the symmetry of the lattice formed by the particles Israelachvili (1992); Zhang & Sham (2003). The interparticle separation can precisely be maneuvered by forming the Langmuir monolayer of the nanoparticles at an interface and changing the surface density. Interestingly, Collier and coworkers have reported a metal-insulator transition in the Langmuir monolayer of hydrophobic silver nanoparticles at the A-W interface Collier et al. (1997); Markovich et al. (1998). They observed a quantum interference between the particles which was governed by interparticle distances. There are few studies on Langmuir monolayer of functionalized metal nanoparticles at the A-W interface Heath et al. (1997); Swami et al. (2003); Greene et al. (2003); Brown et al. (2001); Fukuto et al. (2004). However, the particles studied so far did not show a stable Langmuir monolayer. The important criterion for the formation of stable Langmuir monolayer at the A-W interface is that the particles should be amphiphilic in nature with a proper balance between its hydrophilic and hydrophobic parts Gaines (1966). Accordingly, we synthesized amphiphilic gold nanoparticles (AGN) functionalized with hydroxy terminated alkyl-thiol, and studied the Langmuir film of the particles by surface manometry and microscopy techniques. We find a stable Langmuir monolayer of the AGN at A-W interface. The monolayer exhibits gas, low ordered liquid (L_1), high ordered liquid (L_2), bilayer of L_2 (Bi) and the collapsed states.

The amphiphilic functionalized gold nanoparticles (AGN) were synthesized in the laboratory. The size of the particles was estimated from transmission electron microscope (TEM) images (Figure 13). The particles had a mean core diameter of 5.5 nm with a standard deviation of

±1 nm. The diameter of the AGN for the fully stretched ligands was calculated as 8.4 nm. Hence, the mean cross-sectional area of each particle thus calculated was 55.4 nm^2.

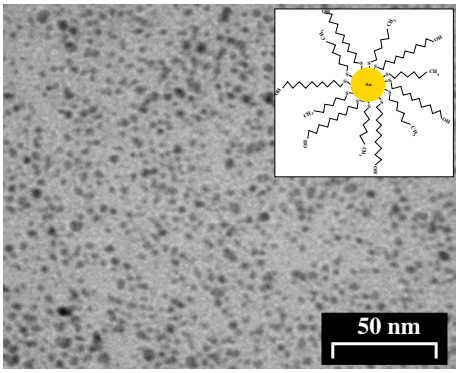

Fig. 13. Transmission electron microscope (Hitachi, H7000, 100 kV) image of the AGN. The solution of the sample of AGN was spread on carbon evaporated copper grid, and the image was scanned after 2 hours. The inset shows structure of an AGN

The surface pressure (π) - area per particle (A_P) isotherms of AGN at different temperatures (Figure 14) show zero surface pressure at very large A_P indicating a coexistence of gas and

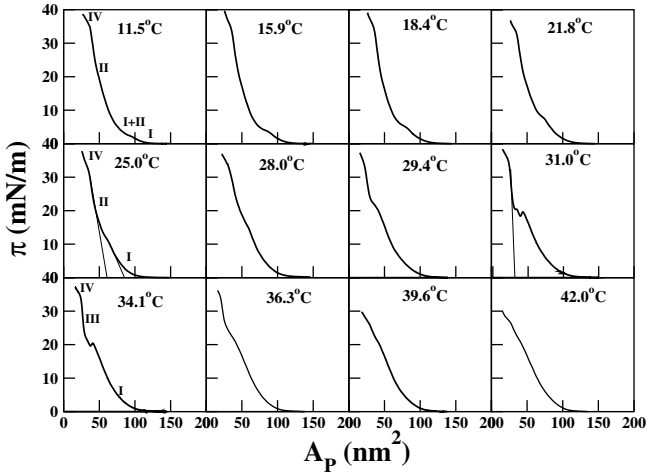

Fig. 14. Surface pressure (π) - area per particle (A_P) isotherms of AGN at different temperatures. The symbols **I, II, III and IV** denote L_1, L_2, Bi and collapsed regions in the isotherms, respectively. The straight lines in the isotherms for temperatures 25 and 31 °C are shown as the extrapolated lines for calculating average area occupied by each particle in the respective phases. The error incurred in such calculation is ±1%. Reprinted with permission. (Gupta & Suresh, 2008)

a low density liquid (L_1) phase. On reducing A_P (monolayer compression), the gas phase disappears, and the isotherms show lift-off area per particle to be around 120 nm^2. On

compressing the monolayer, the isotherms show a slow and gradual rise in surface pressure. This is the pure L_1 phase. The extrapolation of the region of the isotherm to the zero surface pressure on the A_P axis yields the average area occupied by the particles in that particular phase Gaines (1966). The average particle-area in the L_1 phase at 25 °C was 85 nm^2. On compressing the monolayer below 28 °C, the slow and gradual rise in surface pressure is accompanied by a plateau in the isotherms. On further compression, the surface pressure rises sharply till the monolayer collapses at $A_P \sim 36$ nm^2. The region of the isotherm with the sharp rise in surface pressure can correspond to a high density liquid (L_2) phase. At 25 °C, the average particle-area in the L_2 phase was around 61 nm^2. This value nearly corresponds to the mean cross-sectional area of the particles determined through TEM images. The small difference in the value may be due to the poly-dispersity in the size-distribution of the particles. The appearance of plateau in the isotherms suggests a first order phase transition between L_1 and L_2 phases. The coexistence of two phases is denoted as **I+II** in the isotherms. The phase coexisting plateau region decreases with increasing T and finally vanishes above critical temperature (T_c). The T_c was calculated by plotting the enthalpy of the L_1-L_2 transition with respect to T, and extrapolating it to a zero value on the $T-$axis Callen (1985). We obtain a T_c value of 28.4 ^{o}C for this transition. These behaviors have been observed and understood in the case of the standard amphiphilic molecules like phospholipids Mohwald (1995); Birdi (1989); Baoukina et al. (2007). The isotherms indicate a smooth collapse of the monolayer. This may be due to the isotropic shape of the particles. Such smooth collapses were also observed in the case of spherical core functionalised fullerene derivatives Leo et al. (2000); gallani et al. (2002). The reversibility of the isotherms was studied by successive compression and expansion of the monolayer at 25 °C. We find the monolayer to be highly reversible. The stability of the phases were also tested qualitatively by holding the surface pressure at a given value and monitoring the drop in A_P. We find almost no variation in A_P over a long period of time. These observations suggest the monolayer of AGN at the A-W interface to be very stable.

The π-A_P isotherms obtained in the range $28.4 \leq T \leq 36.3$ °C show interesting behaviors. The isotherms show the usual L_1 phase. On reducing the A_P, the L_1 phase appears collapsing by introducing an unstable region in the isotherm. However, on further reducing A_P, the isotherms indicate a steep rise in surface pressure and then smooth collapse like feature. Extrapolating the steep region to the zero surface pressure yields a value of ~ 31 nm^2 at 31 °C. This value is nearly twice than that obtained for the L_2 phase (61 nm^2). Hence, this phase can presumed to be a bilayer (Bi) of L_2 phase. The unstable region of isotherms leading to the transition from L_1 to Bi phase can be considered as a coexistence region. The coexistence region initially increases upto 31 ^{o}C but decreases thereafter until it vanishes above 36.3 ^{o}C. The Bi phase also disappears above 36.3 °C. Thereafter, the monolayer showed gas, L_1 and the collapsed states.

In Brewster angle microscopy, the intensity levels in images depend on surface density and thickness of the films Rivière et al. (1994). The BAM image (Figure 15(a)) at a large A_P shows a coexistence of dark and gray region. The dark region vanishes on compression leading to a uniform gray texture (Figure 15(b)). The gray domains appeared fluidic and mobile under the microscope. The dark region represents gas phase whereas the gray domains correspond to the low density liquid (L_1) phase. The image (Figure 15(c)) corresponding to the plateau region of the isotherms shows bright domains in the gray background. On compression, the bright domains grow at the expense of the gray region leading to a uniform bright texture (Figure 15(d)). The uniform bright texture, obtained in the region **II** of the isotherm, corresponds to the high density liquid (L_2) phase. The coexistence of L_1 and L_2 domains in the

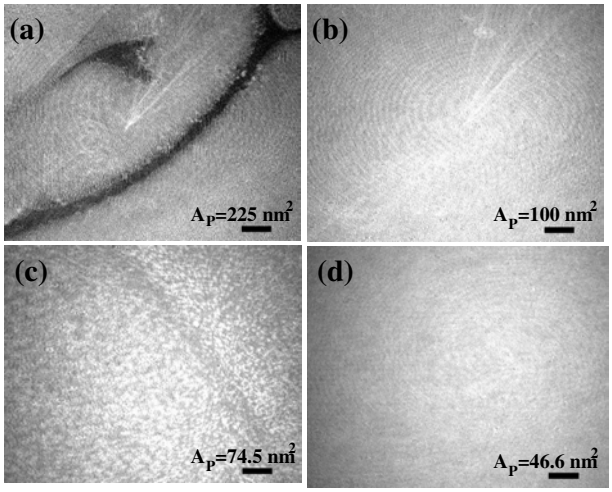

Fig. 15. The BAM images of the monolayer of AGN at 18.4 °C taken at different A_P. (a) a coexistence of dark and gray regions, (b) a uniform gray region, (c) a coexistence of bright domains on the gray background and (d) a uniform bright region. Scale bar = 500 μm. Reprinted with permission. (Gupta & Suresh, 2008)

plateau region of the isotherm establishes a first order phase transition between the phases. The BAM images in the collapsed state showed a wrinkled structure. The wrinkled structure might appear due to folding of the AGN monolayer Lu et al. (2002); Gopal & Lee (2001).

The BAM images of the monolayer of AGN at 31 °C showed the gas (dark region) and L_1 phases (gray region) at large A_P. The gas phase disappears on compressing the monolayer leading to a uniform L_1 phase. The L_1 phase continues to exist till monolayer destabilizes at $A_P \sim 44$ nm^2. Such destabilization leads to the nucleation and growth (Figure 16) of the very bright domains on the gray background. The bright domains grow at the expense of the gray region, finally leading to a uniform bright region. The bright region was obtained in the region of the isotherm corresponding to steep rise in the surface pressure after the destabilization. The bright region corresponds to the bilayer of the L_2 (Bi) phase. The bright region (Bi phase) also collapses on compression leading to a wrinkled structure.

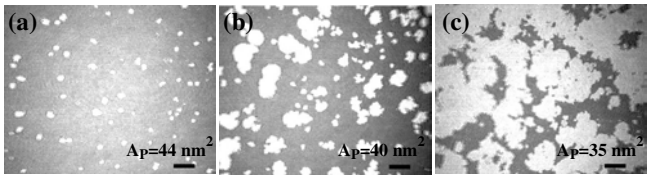

Fig. 16. The BAM images of the monolayer of AGN at 31 °C taken at different A_P. (a)-(c) nucleation and growth of bright domains on the gray background. Scale bar = 500 μm. Reprinted with permission. (Gupta & Suresh, 2008)

Based on our studies, we construct (Figure 17) a phase diagram of the Langmuir monolayer of AGN at the A-W interface.

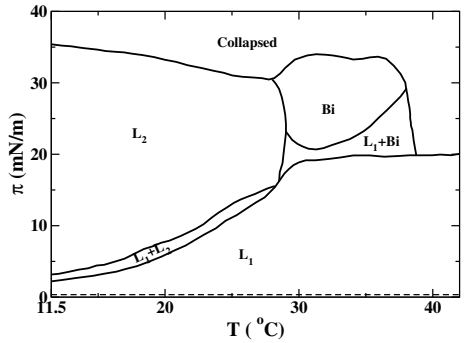

Fig. 17. The phase diagram showing the observed 2D phases of the Langmuir monolayer of AGN at A−W interface. The L_1 and gas phase coexistence was seen even at very large A_P and zero π. This is shown by the dotted line. The L_1, L_2, Bi are the low ordered, high ordered and the bilayer of L_2 phases, respectively. The coexistence of the phases are shown by "+" symbol. Reprinted with permission. (Gupta & Suresh, 2008)

We observed a stable Langmuir monolayer of AGN at the A-W interface. The monolayer exhibits variety of phases like gas, low order liquid (L_1), high ordered liquid (L_2), bilayer of L_2 (Bi) and the collapsed states. The electronic and optical properties of the phases on the different solid substrates will be probed in order to acquaint a better understanding about the structural dependence of the films on such properties.

In the above works, we have observed that an appropriate chemistry of the molecules yields variety of surface phases. Different functional groups in the molecules interact differently. By changing the amphiphilicity of molecules leads to the formation of a stable Langmuir monolayer.

4. Molecular interaction at air-solid interfaces

The variety of surface phases as obtained in the Langmuir films at an A-W interface can be transferred to air-solid (A-S) interface by Langmuir-Blodgett (LB) technique. Such LB films can potentially utilized for the fabrication of devices. The nature of aggregation of the molecules on the surface is important for the device applications. The surface can induce an ordering in the bulk, and hence the material properties can be varied by varying the structure of aggregates on the surface (Ruffieux et al., 2002; Friedlein et al., 2003). The structure of the aggregates on a surface primarily depends on intermolecular and molecule-substrate interactions. In a study we probed the effect of molecule-substrate interaction on the aggregation and nucleation of molecules on substrates which were deposited by LB techniques. We changed the nature of the substrates by chemically treating them to yield a hydrophilic or hydrophobic surfaces. We deposited the LB films of cholesterol on such substrates and studied their nucleation and aggregation using atomic force microscope. The hydrophilic and hydrophobic treatments to the substrates are discussed in details in the article (Gupta & Suresh, 2004). The LB films were transferred to these substrates at a target surface pressure of 30 mN/m. The Langmuir monolayer of Ch exhibits condensed phase at this pressure.

We find that the first layer gets deposited efficiently on both kind of substrates. However, we were not able to transfer more than one layer on hydrophilic substrates. This was due to

the fact that for every upstroke and downstroke of the dipper, the molecules get adsorbed and desorbed by equal amounts. Ch molecule possesses a large hydrophobic sterol moiety. Hence, the interaction between the hydrophilic substrates and the Ch molecules are weak to support the multilayer formation during the LB deposition. On the other hand, the Ch molecules exhibited much better adhesion on hydrophobic glass substrates. During LB transfer on the hydrophobic substrates, we observed the X-type of deposition, where adsorption takes place only during the downstroke. The transfer ratio (τ) data is shown in Figure 18. In each cycle, the two bars represent the τ of one downstroke and one upstroke of deposition. The positive and negative transfer ratio data indicate the adsorption and desorption of the molecules, respectively. We find that the very first monolayer gets deposited efficiently where the τ was always 1 ± 0.02. Contrarily, for upstrokes there was some desorption. During each cycle of deposition, it is clear from the transfer ratio data that downstrokes adsorb the molecules efficiently while the upstrokes desorb fraction of the earlier deposited layers. The desorption increases with increasing number of cycles of deposition. This shows that though

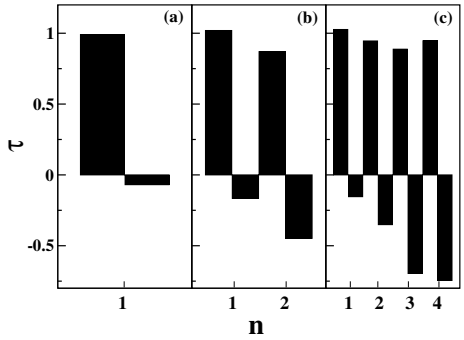

Fig. 18. The transfer ratio (τ) data as a function of number of cycles (n) of LB deposition of Ch on hydrophobic substrates. (a), (b) and (c) represent one, two and four cycles of LB deposition. Reprinted with kind permission of The European Physical Journal.
(Gupta & Suresh, 2004)

the interaction between the hydrophobic substrate and the Ch molecule was strong, the layer to layer interaction was weaker to support multilayer formation. We define the effective adsorption on the substrate as $\eta_n = S_n/\rho_t$ where S_n is the net surface concentration on the substrate after n^{th} cycle and ρ_t is the surface concentration (inverse of A_m) of the monolayer at A-W interface at π_t. The variation of the effective adsorption with the number of cycles of deposition is shown in Figure 19. It is evident from the transfer ratio data (Figure 18) that the desorption becomes significant after the first cycle of deposition. Also, beyond four cycles of deposition, the desorption was almost equal to that of adsorption, resulting in the saturation of effective adsorption, η_n. Hence, it can be inferred that the interaction between the Ch-Ch layers is weaker as compared to that of the hydrophobic substrate-first layer of Ch. The adsorption of one layer of Ch on another layer during LB transfer can lead to defects due to weak layer to layer interaction. These defects can act as nucleation sites for further desorption of the molecules during upstrokes. With increasing cycles of deposition, the filling of the defects and reorganization of the molecules may yield patterns observed in AFM imaging. The AFM images for LB films of Ch on hydrophobic substrates deposited at different cycles show evolution of interesting patterns. The image for first cycle of deposition yields a very uniform texture indicating a uniform film on the surface. The AFM images for second

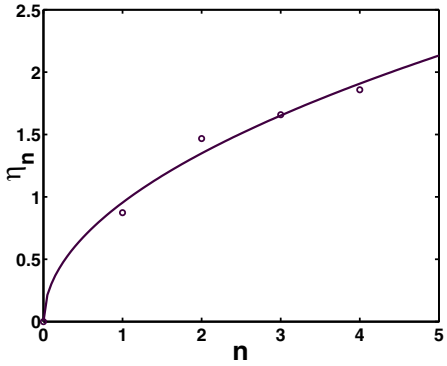

Fig. 19. The effective adsorption η_n is plotted with respect to number of cycles of deposition (n). The experimental data are represented by the open circles (**o**). The continuous line is a guide for the eye. Reprinted with kind permission of The European Physical Journal. (Gupta & Suresh, 2004)

cycle of deposition show elongated domains whereas for the three cycles of deposition, the AFM image shows partial torus shaped domains. Interestingly, the four cycles of deposition reveals uniformly distributed torus-shaped domains (doughnuts) having the outer diameter of about 65 nm and annular width of about 22 nm. The analysis of the phase images indicates the flipping of the Ch molecules. Thus the nature of molecule-substrate interaction play a dominant role not only for multilayer deposition but also the nature of nucleation and aggregation of the molecules on the surface.

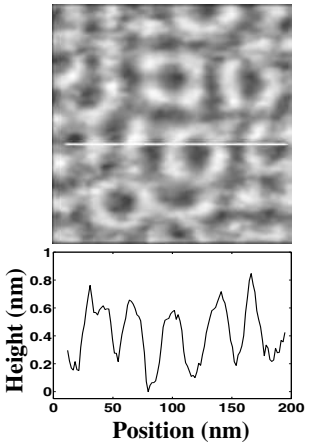

(a)

Fig. 20. AFM image of LB films of cholesterol (Ch) molecules on the hydrophobic substrate deposited during four cycles. The white line on the image is drawn to measure the height variation along it. The corresponding height profiles are shown below the respective images. The image size in each case is 200×200 nm^2. Reprinted with kind permission of The European Physical Journal. (Gupta & Suresh, 2004)

5. Conclusion

We have observed that the stability of Langmuir film can be achieved by changing the amphiphilic balance of the molecules appropriately. In a non-conventional approach, the Langmuir monolayer of hydrophobic molecules can be stabilized by incorporating them in a matrix of a stable monolayer. However, the choice of the stable Langmuir monolayer is such that the dopant mixes readily in the monolayer matrix. The shape and size of nanostructures at A-S interface can be controlled by exploring the possible molecule-substrate and intermolecular interactions.

6. Acknowledgement

We are thankful to University Grants Commission, India for its support under Special Assistance Programme.

7. References

Gaines, G. L. Jr. (1966). *Insoluble Monolayers at Liquid-Gas Interfaces*, Wiley-Interscience, New York.

Adamson A. W. (1990). *Physical Chemistry of Surfaces*, Wiley-Interscience, New York.

Mohwald, H., (1995). *Handbook of Biological Physics*, Lipowsky, R. & Sackmann, E., (Ed.), Elsevier Science, Amsterdam, Vol. 1, Chapter 4.

Smith, R. D. & Berg, J. C. (1980). The collapse of surfactant monolayers at the air-water interface. *J. Colloid Interface Sci.*, Vol. 74, 273-286.

Ramakrishnan, V.; Costa, M. D.; Ganesh, K. N. & Sastry, M. (2002). PNA-DNA hybridization at the air-water interface in the presence of octadecylamine Langmuir monolayers. *Langmuir*, Vol. 18, 6307-6311.

Goodrich, F. C. (1957). *Proceedings of the 2nd International Congress on Surface Activity*. Schulman J. H. (ed.), Butterworths, London, Vol. 1, 85.

Seoane, R.; Dynarowicz-tstka, P.; Miñones Jr., J. & Rey-Gòmez-Serranillos, I. (2001). Mixed Langmuir monolayers of cholesterol and essential fatty acids.*Colloid Polym. Sci.*, Vol. 279, 562-570.

Tscharner V. and McConnell, H. M. (1981). An alternative view of phospholipid phase behavior at the air-water interface. Microscope and film balance studies.*Biophys. J.*, Vol. 36, 409-419.

Hönig, D. & Möbius, D. (1991). Direct visualization of monolayers at the air-water interface by Brewster angle microscopy. *J. Phys. Chem.*, Vol. 95, 4590-4592.

Hénon, S. & Meunier, J. (1991). Microscope at the Brewster angle: Direct observation of first-order phase transitions in monolayers. *Rev. Sci. Instrum.*, Vol. 62, 936-939.

S. Rivière, S. Hénon, J. Meunier, D. K. Schwartz, M.-W. Tsao, and C. M. Knobler, C. M. (1994). Textures and phase transitions in Langmuir monolayers of fatty acids. A comparative Brewster angle microscope and polarized fluorescence microscope study. *J. Chem. Phys.*, Vol. 101, 10045-10051.

Roberts, G. (1990). *Langmuir-Blodgett Films*, Plenum, New York.

Binning, G.; Rohrer, H.; Geber, Ch. & Weibel, E. (1982). Surface studies by scanning tunneling microscopy. *Phys. Rev. Lett.*, Vol. 49, 57-61.

Binning, G.; Quate, C. F. & Gerber, Ch. (1986). Atomic force microscope. *Phys. Rev. Lett.*, Vol. 56, 930-933.

Tabe, Y; Yamamoto, T.; Nishiyama, I.; Aoki, K. M.; Yoneya, M. & Yokoyama, H.(2002). Can hydrophobic oils spread on water as condensed Langmuir monolayers? *J. Phys. Chem. B*, Vol. 106, 12089-12092.

Gaines, G. L. (1991). Surface activity of semifluorinated alkanes: F(CF2)m(CH2)nH. *Langmuir*, Vol. 7, 3054-3056.

Abed, A. El; Fauré, M-C.; Pouzet, E. & Abillon, O. (2002). Experimental evidence for an original two-dimensional phase structure: An antiparallel semifluorinated monolayer at the air-water interface. *Phys. Rev. E*, Vol. 65, 051603-4.

Huo, Q.; Russev, S.; Hasegawa, T.; Nishijo, J.; Umemura, J.; Puccetti, G.; Russell, K. C. & Leblanc, R. M. (2000) A Langmuir monolayer with a nontraditional molecular architecture. *J. Am. Chem. Soc.*, Vol. 122, 7890-7897.

Yang,Z. P.; Engquist, I.; Kauffmann,J. -M.; & Liedberg, B. (1996). Thiocholesterol on gold: A nanoporous molecular assembly . *Langmuir*, Vol. 12, 1704-1707.

Slotte, J. P. & Mattjus, P. (1995). Visualization of lateral phases in cholesterol and phosphatidylcholine monolayers at the air water interface - a comparative study with two different reporter molecules. *Biochim. Biophys. Acta*, Vol. 1254, 22-29.

Lafont, S.; Rapaport,H.; Sömjen, G. J.; Renault, A.; Howes, P.B.; Kjaer, K.; Als-Nielsen, J.; Leiserowitz, L. & Lahav, M. (1998). Monitoring the nucleation of crystalline films of cholesterol on water and in the presence of phospholipid. *J. Phys. Chem. B*, Vol. 102, 761-765.

Bilewicz, R. & Majda, M. (1991). Monomolecular Langmuir-Blodgett films at electrodes. Formation of passivating monolayers and incorporation of electroactive reagents, *Langmuir*, Vol. 7, 2794-2802.

Silva, A. M. G.; Guerreiro, J. C.; Rodrigues, N. G. & Rodrigues, T. O. (1996). Mixed monolayers of heptadecanoic acid with chlorohexadecane and bromohexadecane. Effects of temperature and of metal ions in the subphase,*Langmuir*, Vol. 12, 4442-4448.

Wang, H.; Ozaki, Y. & Iriyama, K. (2000). An infrared spectroscopy study on molecular orientation and structure in mixed Langmuir-Blodgett films of 2-octadecyl-7,7,8,8-tetracyanoquinodimethane and deuterated stearic acid: Phase separation and freezing-in effects of the fatty acid domains, *Langmuir*, Vol. 16, 5142-5147.

Viswanath, P. & Suresh, K. A. (2004). Photoinduced phase separation and miscibility in the condensed phase of a mixed Langmuir monolayer, *Langmuir*, Vol. 20, 8149-8154.

Viswanath, P. & Suresh, K. A. (2003). Polar head group interactions in mixed Langmuir monolayers, *Phys. Rev. E*, Vol. 67, 061604-8.

Gupta, R. K. & Suresh K. A. (2008). Stabilization of Langmuir monolayer of hydrophobic thiocholesterol molecules. *Colloids & Surfaces A:Physicochemical and Engineering Aspects*, Vol. 320, 233-239.

Li, M. Y.; Acero, A. A.; Huang, Z. & Rice, S. A. (1994). Formation of an ordered Langmuir monolayer by a non-polar chain molecule. *Nature*, Vol. 367, 151-153.

Tkachenko,A. V. & Rabin, Y. (1996). Fluctuation-stabilized surface freezing of chain molecules. *Phys. Rev. Lett.*, Vol. 76, 2527-2530.

Jensen, T. R.; Jensen, M. Ø.; Reitzel, N.; Balashev, K.; Peters, G. H.; Kjaer, K. & Bjørnholm, T. (2003). Water in contact with extended hydrophobic surfaces: Direct evidence of weak tweeting. *Phys. Rev. Lett.*, Vol. 90, 086101-4.

Jensen, M. Ø.; Mauritsen, O. G. & Peters, G. H. (2004). The hydrophobic effect: Molecular dynamics simulations of water confined between extended hydrophobic and hydrophilic surfaces. *J. Chem. Phys.*, Vol. 120, 9729-9744.

Israelachvili, J. N., *Intermolecular and Surface Forces : With Applications to Colloidal and Biological Systems* (Academic Press, London, 1992).

Zhang, P., & Sham, T. K. (2003). X-Ray studies of the structure and electronic behavior of alkanethiolate-capped gold nanoparticles: The interplay of size and surface effects. *Phys. Rev. Lett.*, Vol. 90, 245502-4.

Collier, C. P.;Saykally, R. J.; Shiang, J. J.; Henrichs, S. E. & Heath, J. R. (1997). Reversible tuning of silver quantum dot monolayers through the metal-insulator transition. *Science*, Vol. **277**, 1978-1981.

Markovich, G.; Collier, C. P. & Heath, J. R. (1998). Reversible metal-insulator transition in ordered metal nanocrystal monolayers observed by impedance spectroscopy. *Phys. Rev. Lett*, Vol. 80, 3807-3810.

Heath, J. R.; Knobler, C. M. & Leff, D. V. (1997). Pressure/Temperature phase diagrams and superlattices of organically functionalized metal nanocrystal monolayers: The influence of particle size, size distribution, and surface passivant. *J. Phys. Chem. B*, Vol. 101, 189-197.

Swami, A.; Kumar, A.; Selvakannan, P. R.;Mandal, S.; & Sastry, M. (2003). Langmuir-Blodgett films of laurylamine-modified hydrophobic gold nanoparticles organized at the air-water interface. *J. Col. Int. Sci.*, Vol. 260, 367-373.

Greene, I. A.; Wu, F.; Zhang, J. Z. & Chen, S. (2003). Electronic conductivity of semiconductor nanoparticle monolayers at the air-water interface. *J. Phys. Chem. B*, Vol. 107, 5733-5739.

Brown, J. J.; Porter, J. A.; Daghlian, C. P. & Gibson, U. J. (2001). Ordered arrays of amphiphilic gold nanoparticles in langmuir monolayers. *Langmuir*, Vol. 17, 7966-7969.

Fukuto, M.; Heilmann, R. K.; Pershan, P. S.; Badia, A. & Lennox, R. B. (2004). Monolayer/bilayer transition in Langmuir films of derivatized gold nanoparticles at the gas/water interface: An x-ray scattering study. *J. Chem. Phys.*, Vol. 120, 3446-3459.

Callen, H. B. (1985). *Thermodynamics and an Introduction to Thermostatistics*, John Wiley & Sons, New York.

Birdi, K. S. (1989). *Lipid and Biopolymer Monolayers at Liquid Interfaces*, Plenum, New York.

Baoukina, S.; Monticelli, L.; Marrink, S. J. & Tieleman, D. P. (2007). Pressure-area isotherm of a lipid monolayer from molecular dynamics simulations. *Langmuir*, Vol. 23, 12617-12623.

Leo, L.; Mele, G.; Rosso, G.; Valli, L.; Vasapollo, G.; Guldi, D. M. & Mascolo, G. (2000). Interfacial properties of substituted fulleropyrrolidines on the water surface. *Langmuir*, Vol. 16, 4599-4606.

Gallani, J.; Felder, D.; Guillon, D.; Heinrich, B. & Nierengarten, J. (2002). Micelle formation in Langmuir films of C_{60} derivatives. *Langmuir*, Vol. 18, 2908-2913.

Gupta, R. K. & Suresh, K. A. (2008). Monolayer of amphiphilic functionalized gold nanoparticles at an air-water interface. *Phys. Rev. E*, Vol. 78, 032601-4.

Lu, W.; Knobler, C. M.; Bruinsma, R. F.; Twardos, M. & Dennin, M. (2002). Folding Langmuir monolayer. *Phys. Rev. Lett.*, Vol. 89, 146107-4.

Gopal, A. & Lee, K. Y. C. (2001). Morphology and collapse transitions in binary phospholipid monolayers. *J. Phys. Chem. B*, Vol. 105, 10348-10354.

Ruffieux, P.; Gröning, O.; Bielmann, M.; Simpson, C.; Müllen, K.; Schlapbach, L. & Gröning, P. (2002). Supramolecular columns of hexabenzocoronenes on copper and gold (111) surfaces. *Phys. Rev. B*, Vol. 66, 073409-4.

Friedlein, R.; Crispin, X.; Simpson, C. D.; Watson, M. D.; Jäckel, F.; Osikowicz, W.; Marciniak, S.; de Jong, M. P.; Samori, P.; Jönsson, S. K. M.; Fahlman, M.; Müllen, K.; Rabe, J. P. & Salaneck, W. R. (2003). Electronic structure of highly ordered films of self-assembled graphitic nanocolumns. *Phys. Rev. B*, Vol. 68, 195414-7.

Gupta, R. K. & Suresh, K. A. (2004). AFM studies on Langmuir-Blodgett films of cholesterol. *Euro. Phys. J. E*, Vol. 14, 35-42.

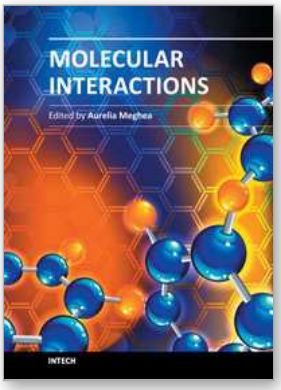

Molecular Interactions

Edited by Prof. Aurelia Meghea

ISBN 978-953-51-0079-9
Hard cover, 400 pages
Publisher InTech
Published online 29, February, 2012
Published in print edition February, 2012

In a classical approach materials science is mainly dealing with interatomic interactions within molecules, without paying much interest on weak intermolecular interactions. However, the variety of structures actually is the result of weak ordering because of noncovalent interactions. Indeed, for self-assembly to be possible in soft materials, it is evident that forces between molecules must be much weaker than covalent bonds between the atoms of a molecule. The weak intermolecular interactions responsible for molecular ordering in soft materials include hydrogen bonds, coordination bonds in ligands and complexes, ionic and dipolar interactions, van der Waals forces, and hydrophobic interactions. Recent evolutions in nanosciences and nanotechnologies provide strong arguments to support the opportunity and importance of the topics approached in this book, the fundamental and applicative aspects related to molecular interactions being of large interest in both research and innovative environments. We expect this book to have a strong impact at various education and research training levels, for young and experienced researchers from both academia and industry.

INTECH
open science | open minds

InTech Europe
University Campus STeP Ri
Slavka Krautzeka 83/A
51000 Rijeka, Croatia
Phone: +385 (51) 770 447
Fax: +385 (51) 686 166
www.intechopen.com

InTech China
Unit 405, Office Block, Hotel Equatorial Shanghai
No.65, Yan An Road (West), Shanghai, 200040, China
中国上海市延安西路65号上海国际贵都大饭店办公楼405单元
Phone: +86-21-62489820
Fax: +86-21-62489821